Journal of Organometallic Chemistry 693 (2008) 2937–2941

Contents lists available at ScienceDirect

Journal of Organometallic Chemistry

journal homepage: www.elsevier.com/locate/jorganchem

The differences in solid state structures of *C,N*-chelated *n*butyltin(IV) fluorides

Petr Švec [a], Zdeňka Padělková [a], Zdeněk Černošek [a], Frank De Proft [b], Aleš Růžička [a,*]

[a] Department of General and Inorganic Chemistry, Faculty of Chemical Technology, University of Pardubice, nám. Čs. legií 565, CZ-532 10, Pardubice, Czech Republic
[b] Eenheid Algemene Chemie (ALGC), Department of Chemistry (DSCH), Faculty of Sciences, Vrije Universiteit Brussel (VUB), Pleinlaan 2, B-1050 Brussels, Belgium

ARTICLE INFO

Article history:
Received 6 March 2008
Received in revised form 26 May 2008
Accepted 5 June 2008
Available online 11 June 2008

Keywords:
Organotin(IV) fluorides
CN-ligand
Structure

ABSTRACT

The solid state structures of products of fluorination of $L^{CN}nBuSnCl_2$ (where L^{CN} is 2-[$(CH_3)_2NCH_2$]C_6H_4–) by different methods are reported. The reaction of 3 equiv. of $[NH_4]^+[L^{CN}nBuSnF_3]^-$ and $Pr(OTf)_3$ led to dimeric arrangement $[L^{CN}nBuSnF(\mu\text{-}F)_2SnL^{CN}nBuF]\cdot 2HOTf$. Two different polymorphs of polymeric $[L^{CN}nBuSnF_2]_n$ have been obtained by crystallization. Prepared compounds were studied by X-ray crystallographic methods, DSC and theoretical calculations at the B3LYP/LANL2DZ level.

1. Introduction

The tri- and diorganotin(IV) fluorides were described as insoluble polymeric species with changeable composition and properties [1,2]. Two- or three-dimensional structures connected via F–Sn–F bridges have been determined or suggested for majority of these compounds. This aggregation can be prevented in the case of triorganotin fluorides either by use of bulky substituents and/or donor ligands especially chelating ones in both cases [3–9].

We have reported previously on monomeric triorganotin(IV) fluorides of general formula $L^{CN}R_2SnF$, where L^{CN} is {2-[$(CH_3)_2$-NCH_2]C_6H_4}$^-$ and R is alkyl (Me, *n*Bu, *t*Bu) or aryl (Ph) groups of different steric bulk and electronic properties [10] which can be used for metathetical halide for fluoride exchange reactions for inorganic salts or complexes, chlorosilanes, chlorophosphines and different kinds of organometallic compounds [11]. We also reported the first monomeric diorganotin(IV) difluoride wearing the same ligands ($L_2^{CN}SnF_2$ (**1**) with sixfold coordinated tin centre and *C,C-transoid* geometry – Sn1–F1 1.981(1), Sn1–F2 1.991(1), Sn1–N1 2.496(2), Sn1–N2 2.597(1)) [12,13] having no interaction of tin atom with another atom from adjacent molecule. When only one ligand is used ($L^{CN}RSnF_2$; R = Ph [12], *n*Bu [11a], F [14]) the di- or monoorganotin(IV) fluorides are presumably tri- or tetranuclear species with rather low solubility in common organic solvents and we used them recently as a part of selective and sensitive carriers for fluoride ion recognition [15].

The investigation of $L^{CN}nBuSnCl_2$ (**2**) [16,17] and products of its fluorination [11a] showed interesting differences between structures in solution and in the solid state. Compound **2** is monomeric in solution of non-coordinating solvent such as $CDCl_3$ with fivefold coordinated tin i.e., two carbon and one of chlorine atoms in equatorial positions and both nitrogen and the remaining chlorine atom in axial ones. The six-coordinated tin has been found in the coordinating solvents such as DMSO-d_6. The tendency of tin atom to increase the coordination number is clearly seen in the solid state as well. The solid state structure of **2** (Fig. 1) can be described as a polymer with Cl–Sn–Cl zig-zag chain having two different structural motifs of a mononuclear unit. The main difference is the shape of the *n*-butyl substituent and the Sn–Cl bond lengths. The four different Cl atoms are present; Sn1–Cl(bridging-a) 2.4686(10) Å and Sn2–Cl(bridging) 3.4440(11) Å), Sn1–Cl(terminal-a) 2.3877(11) Å, Sn2–Cl(bridging-b) 2.4620(10) Å and Sn1′–Cl3 3.6256(11) Å), iv) Sn2–Cl(terminal-b) 2.3926(10) Å.

Two different methods were used for replacing chlorine by fluorine atom(s) in **2**. The first method is based on the known fluorination ability of $L^{CN}nBu_2SnF$ and the second one is reaction with dried NH_4F (excess) in dichloromethane under an argon atmosphere yielding the same species or ionic stannates ($[NH_4]^+[L^{CN}nBuSnF_3]^-$). In chloroform, a polymeric structure is probably retained which is also supported by the ^{19}F NMR spectra, where two very broad signals were found at room temperature and no signal was observed at 220 K. In weakly coordinating solvents such as nitrobenzene or acetonitrile, the tetrameric structure was deduced from ESI-MS measurements. The structure in DMSO is monomeric with dynamically exchanging fluorine atoms (from axial to equatorial position of trigonal bipyramid).

Although a large number of attempts have been made, no solid state structure of these complexes was determined up to now. In this paper, we would like to communicate different solid state

* Corresponding author. Tel.: +420 466037151; fax: +420 466037068.
E-mail address: ales.ruzicka@upce.cz (A. Růžička).

0022-328X/$ - see front matter © 2008 Published by Elsevier B.V.
doi:10.1016/j.jorganchem.2008.06.010

Table 1
Selected crystallographic data for **3a–c**

Compound	**3a**	**3b**	**3c**
Empirical formula	$C_{28}H_{48}F_{10}N_2O_6S_2Sn_2$	$C_{13}H_{21}F_2NSn$	$C_{13}H_{21}F_2NSn$
Crystal system	Triclinic	Triclinic	Triclinic
Space group	$P\bar{1}$	$P\bar{1}$	$P\bar{1}$
a (Å)	10.0890(11)	8.4120(5)	4.276(2)
b (Å)	10.7420(8)	8.563(2)	8.4020(12)
c (Å)	11.4180(12)	10.0910(16)	9.453(6)
α (°)	108.455(7)	108.690(15)	87.65(3)
β (°)	95.985(7)	90.636(9)	83.98(5)
γ (°)	117.955(6)	92.476(11)	87.31(3)
Z	1	2	1
V (Å^3)	988.57(17)	687.7(2)	337.2(3)
D_c (g cm^{-3})	1.680	1.748	1.734
Crystal size (mm)	0.293 × 0.226 × 0.096	0.193 × 0.140 × 0.084	0.119 × 0.098 × 0.043
Crystal shape	Block	Needle	Block
μ (mm^{-1})	1.455	1.866	1.898
F(000)	500	362	178
h, k, l range	−13, 13, −12, 13, −14, 14	−10, 10, −11, 11, −13, 13	−5, 5, −10, 10, −12, 12
θ Range (°)	2.36–27.50	2.13–27.49	3.20–27.49
Temperature	150(1)	200(1)	100(1)
Reflections measured	18700	12630	5844
Independent (R_{int})[a]	8450 (0.061)	5667 (0.065)	2840 (0.068)
Observed [$I>2\sigma(I)$]	7587	4243	2835
Parameters refined	441	313	149
Max/min τ (e Å^{-3})	1.280/−1.095	0.909/−1.270	2.511/−1.254
Goodness-of-fit[b]	1.058	1.149	1.075
R^c/wR^c	0.0431/0.1059	0.0380/0.0955	0.0513/0.1323

[a] $R_{int} = \sum|F_o^2 - F_{o,mean}^2|/\sum F_o^2$.
[b] $S = [\sum(w(F_o^2 - F_c^2)^2)/(N_{diffrs} - N_{params})]^{1/2}$.
[c] Weighting scheme: $w = [\sigma^2(F_o^2) + (w_1P)^2 + w_2P]^{-1}$, where $P = [\max(F_o^2) + 2F_c^2]$, $R(F) = \sum||F_o| - |F_c||/\sum|F_o|$, $wR(F^2) = [\sum(w(F_o^2 - F_c^{2})^2)/(\sum w(F_o^2)^2)]^{1/2}$.

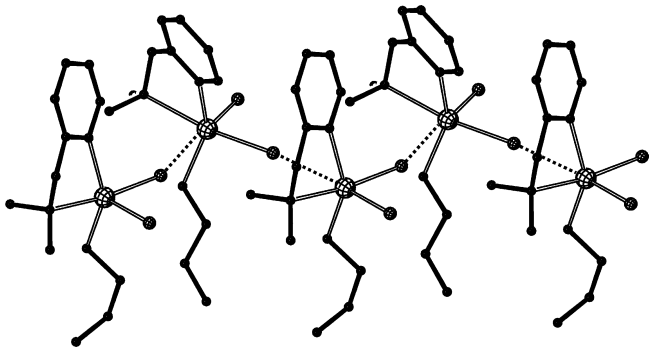

Fig. 1. Supramolecular architecture of **2**.

structures determined by X-ray techniques supported by theory and DSC techniques.

2. Results and discussion

The dimeric structure **3a** ([L^{CN}*n*BuSnF(μ-F)$_2$SnL^{CN}*n*BuF] · 2HOTf (Fig. 2)) has been obtained by crystallization of reaction mixture of 3 equiv. of [NH$_4$]$^+$[L^{CN}*n*BuSnF$_3$]$^-$ and Pr(OTf)$_3$. This reaction has been carried out in order to prepare species with Sn–F–lanthanide structural motif analogous to complexes of Demsar's praseodymium and neodymium fluorotitanates [18], but **3a** and white insoluble powder, probably a praseodimium fluoride, were the only isolable products. When **3a** was dissolved in non-coordinating solvent, the same spectra were obtained as for previously reported products of fluorination of **2** [11a]. This can be explained by the hypothesis that **3a** exists only in the solid state. The basic building block of the structure of **3a** (Fig. 2) consists of two tin atoms bridged by nearly symmetrical bridge of two fluorine atoms (Sn2–F2 2.146(12), Sn2–F3 2.128(8), F2–Sn1 F3 73.3(3), F2–Sn2–F3 72.1(3)). Each tin atom is six-coordinated with two carbon

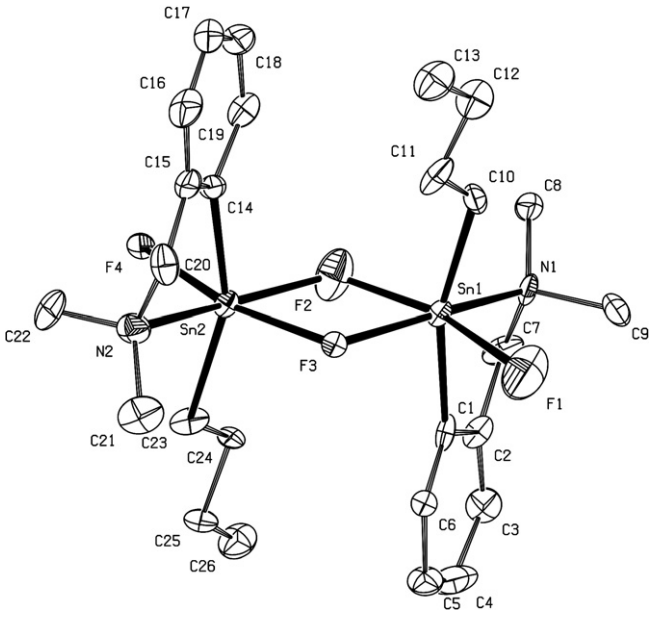

Fig. 2. ORTEP plot of molecule **3a** showing 50% probability displacement ellipsoid and the atom numbering scheme. Hydrogen atoms and trifluoromethane sulphonic acid moieties were omitted for clarity. The selected bonding lengths (Å) and angles (deg): Sn1–C10 2.090(14), Sn1–F2 2.107(12), Sn1–F3 2.106(8), Sn1–C1 2.143(17), Sn1–F1 2.352(12), Sn1–N1 2.434(14), Sn2–C14 2.089(15), Sn2–F2 2.146(12), Sn2–F3 2.128(8), Sn2–C23 2.147(12), Sn2–F4 2.348(6), Sn2–N2 2.465(15), F2–Sn1–F3 73.3(3), C10–Sn1–C1 161.7(5), F2–Sn1–F1 161.9(4), F3–Sn1–F1 88.7(4), F3–Sn1–N1 160.4(4), F2–Sn2–F3 72.1(3), F2–Sn2–F4 89.2(3), F3–Sn2–F4 161.3(2), F2–Sn2–N2 162.3(5).

atoms of ligand and butyl moieties in mutually trans positions (C10–Sn1–C1 161.7(5)), two bridging fluorine atoms, one coordinated nitrogen atom and one terminal fluorine atom with extremely long Sn–F distance(s) (Sn1–F1 2.352(12) and Sn2–F4

2.348(6)). Each nitrogen atom is located in *trans* position (Sn1–N1 2.434(14) and Sn2–N2 2.465(15)) to one of bridging fluorine atoms and the second bridging fluorine atom is trans to the terminal one (F2–Sn1–F1 161.9(4), F3–Sn1–N1 160.4(4), F3–Sn2–F4 161.3(2), F2–Sn2–N2 162.3(5)). The hypothesis that **3a** exists only in the solid state is supported by the stabilization of **3a** into the linear motifs connected by hydrogen bridging via trifluoromethane sulphonic acid moieties (Fig. 3).

When the product of fluorination of **2** has been crystallized from methanol solution crystals of **3b** (Figs. 4 and 5) were obtained. The almost linear polymeric structure where the six-coordinated tin atoms are connected by one fluorine bridge is very different of previously found structure of **2**, where a zig-zag chain is taking place, dimeric **3a** or monomeric **1**. This fact is demonstrated mainly in differences in Sn-F bond lengths and Sn–F–Sn angles (Fig. 5). Both distances of the terminal and bridging fluorine to tin atoms are comparable to the values found in the literature and for example for **1** [12]. The non-equal distances for bridging Sn-F bonds were found. Very strong intramolecular connection Sn–N comparable to monomeric triorganotin fluorides [10] or monoorganotin halides [14] was found for all compounds.

The different polymorph **3c** (Figs. 4 and 5) of the same compound has been obtained from methanolic solution of fluorination product of **2** and ammonium fluoride in the first crystallization crop. The second crop gave the mixture of **3c** (needles) and **3b** (blocks) in approx. 4:1 ratio. The structure of **3c** is similar to **3b** from the point of view of found main interatomic distances and angles (Fig. 5) but in the closer investigation of polymeric chain there is the major difference in mutual orientation of butyl and ligand moieties through this chain. While in **3c** is the same orientation of butyl moieties in **3b** is the opposite one (ca. 180° rotated perpendicularly to polymer axis). This phenomenon can be interpreted either by the polymer chemistry or inorganic chemistry nomenclature as isotactic (**3c**) and syndiotactic (**3b**) polymers or infinite chain of optical (in octahedral coordination vicinity of tin atoms) A,C (alternating) or A,A isomers.

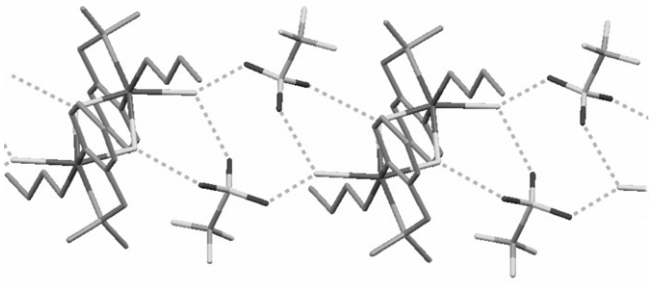

Fig. 3. View of H-bonding in **3a** with O-F distances being 2.749(3), 2.774(1), and 2.774(3) Å.

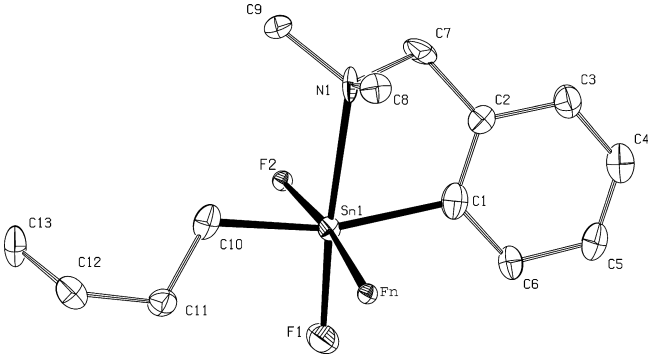

Fig. 4. ORTEP view of one of building blocks of **3b** (n = 3) or **3c** (n = 2a) showing 50% probability displacement ellipsoid and the atom numbering scheme. Hydrogen atoms were omitted for clarity.

When the structure of **3c** was determined at higher temperatures a phenomenon of slight change of polymer from 'rod-like' to 'zig-zag' one is observed (increase of residual electronic maxima in the direction of proposed zig-zag chain, for a similar change from polymeric to monomeric structure with temperature change see Ref. [19]). On the other hand, isomer **3b** retained unchanged in the range of 100–250 K. This is probably caused by a repulsion of π-electrons of Ph rings in **3c**.

The difference between these isomers (**3b** and **3c**) is also reflected in different patterns of DSC curves (Fig. 6). Starting at 196 °C an exothermic process with enthalpy change −18 J/g can be seen for both isomers. Using optical microscopy we have found gradual crystal growth in the temperature range 196–239 °C, immediately before crystall melt accompanied at the same time by decomposition. Starting temperatures and total enthalpy changes of melting and decomposition were found: 239 °C and −278 J/g for isomer **3b**, and 244 °C and −780 J/g for isomer **3c**, see Fig. 6. As one can see on Fig. 6, the isomer **3c** contains observable amout of isomer **3b** manifesting itself by small exothermic peak at 257 °C. More complicated peak shape of melting and decomposition of isomer **3c** is not fully clear up to now.

The pathway going from monomeric compound **1**, through dimeric **3a** and a monomer-like **2** to polymeric **3b** and **3c** in both rod-like and zig-zag version have been examined also at the theory level. The geometries of all compounds were optimized at the B3LYP [20]/LANL2DZ [21,22] level of theory starting from the different crystal structures obtained. It has previously been shown that this level of theory is capable of qualitatively describing intramolecular interactions in organotin compounds [23].

Tables S1–S5 (see Supplementary material) provide a comparison of a series of different relevant geometrical parameters for the different compound considered in this work. In the case of $L_2^{CN}SnF_2$ (**1**) (Table S1) it can be seen that the agreement of the computed distances and bond angles with the values from the crystal structures is very good in the majority of cases; the largest difference occurs in the case of the F–Sn–F angle, where the computed angle is somewhat larger than the experimental one. The similar situation appeared in the case of staring compound **2**, where only the small differences between calculated and measured distances and angles are caused by weak van der Waals interactions in the solid state (Table S2). When going to the dimer **3a** (Table S3), F–Sn–F angle decreases, the decrease being larger in the case of the computed structures. In the dimer, the largest differences between the computed and experimental values are related to both the F–Sn bond distances and the F–Sn–F bond angles. The Sn–F distances for the atoms involved in the bridge are much more asymmetric for the computed structures than in the case of the crystal structures, where these values are very close to one another. On of the two calculated distances however is always very close to the experimental distance. As can be seen, the change in the Sn–F distances for the fluorine atoms not involved in the bridge when going from the monomeric $L_2^{CN}SnF_2$ to the dimer is much less pronounced for the calculated values than for the experimental ones.

Next, we consider the optimized geometry for the syndio (**3b**) and isotactic form **3c** (Tables 4S and 5S). As can be seen, most computed bond distances and angles are in reasonable agreement with the experimental values. The largest deviation occurs for the distance between Sn1 and F2. For **3c**, the Sn1–F2–Sn1a angle amounts to the value of 170.98° in the crystal structure and decreases 153.50°, indicating a more zig-zag character of the gas phase structure as compared to the solid phase structure. This is accompanied by an increased degree of atacticity in the gas phase structure.

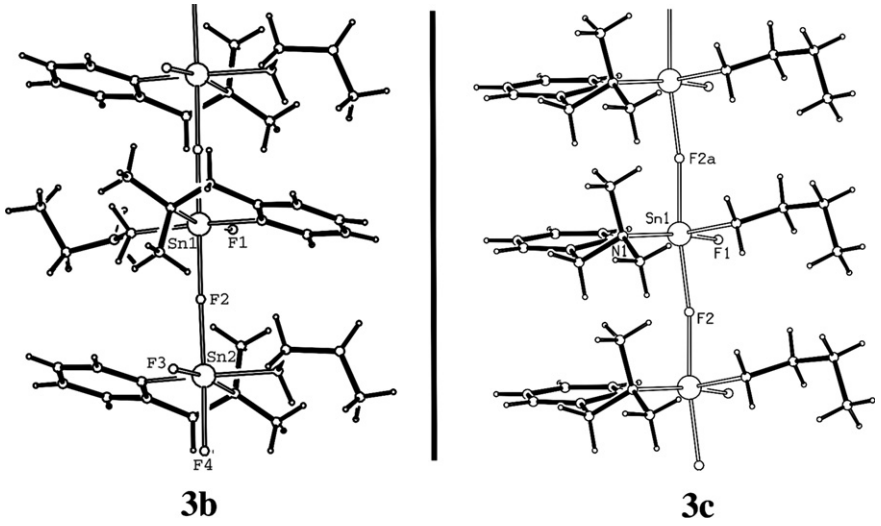

Fig. 5. Comparative view of **3b** and **3c**. Selected bond lengths (Å) and angles (deg) for **3b**: Sn1–F1 1.972(9), Sn1–C1 2.133(15), Sn1–F2 2.13(3), Sn1–C10 2.162(15), Sn1–F4 2.17(3), Sn1–N1 2.574(14), Sn2–C23 2.026(18), Sn2–F3 2.041(10), Sn2–C14 2.081(17), Sn2–F4 2.13(3), Sn2–F2 2.13(3), Sn2–N2 2.427(12), F1–Sn1–F2 87.7(10), C1–Sn1–C10 160.2(5), F1–Sn1–F4 89.2(9), F2–Sn1–F4 176.8(18), F1–Sn1–N1 172.0(5), C23–Sn2–C14 165.9(7), F3–Sn2–F4 93.0(9), F3–Sn2–F2 88.5(10), C14–Sn2–F2 91.5(11), F4–Sn2–F2 178.3(18), F3–Sn2–N2 169.2(4), Sn2–F2–Sn1 177.9(19), Sn2–F4–Sn1 177.5(18). For **3c**: Sn1–C1 2.111(12), Sn1–F1 1.966(8), Sn1–F2 2.168(8), Sn1–F2a 2.121(8), Sn1–C10 2.131(12), Sn1–N1 2.470(12), F1–Sn1–F2 84.8(3), F1–Sn1–F2a 86.7(3), F2–Sn1–F2a 171.0(3), C1–Sn1–C10 162.0(4), F1–Sn1–N1 171.4(4), Sn1–F2–Sn1a 171.0(3).

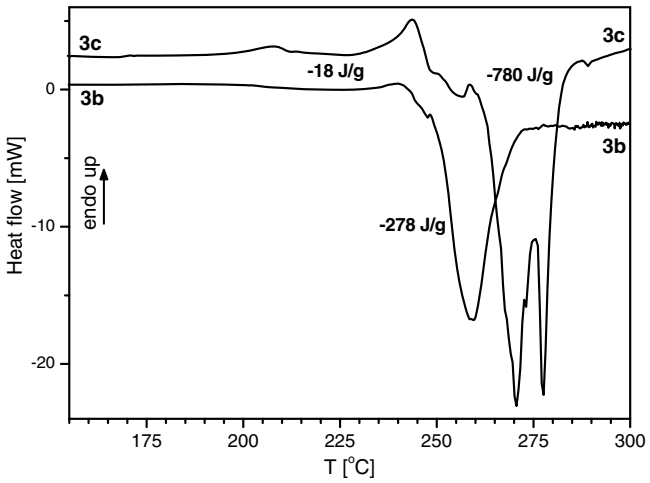

Fig. 6. Observed DSC parameters for **3b** and **3c**.

3. Experimental

$L^{CN}nBuSnCl_2$ (**2**) was prepared and fluorinated as published elsewhere [16,17,11a]. All solvents and starting compounds were obtained from commercial sources (Aldrich). THF was dried by distillation from sodium–potassium alloy, dichloromethane from calcium hydride and degassed.

3.1. $[L^{CN}nBuSnF(\mu\text{-}F)_2SnL^{CN}nBuF] \cdot 2HOTf$ (3a)

The $Pr(OTf)_3$ (0.033 g, 0.056 mmol) was dissolved in 15 ml of THF and 3 equiv. of $[NH_4]^+[L^{CN}nBuSnF_3]^-$ (0.065 g, 0.169 mmol) were added. The reaction mixture was stirred overnight. Afterwards, the reaction mixture was reduced to approx. half of its original volume, the soluble part was filtered off and the volatiles were *vacuo* removed. The product was dissolved in dichloromethane. Colourless single crystals were obtained from this solution at −30 °C. Yield 0.029 g (52%). M.p. 202–203 °C. Elemental Anal. Calc. for $C_{28}H_{44}F_{10}N_2O_6S_2Sn_2$ (996.17): C, 33.76; H, 4.45; N, 2.81; S, 6.44. Found: C, 33.65; H, 4.58; N, 2.90; S, 6.35%.

3.2. NMR spectroscopy

The NMR spectra were recorded as solutions in methanol-d_4, or $CDCl_3$ on a Bruker Avance 500 spectrometer (equipped with *Z*-gradient 5 mm probe) at 300, 250 or 220 K ^1H (500.13 MHz), $^{119}Sn\{^1H\}$ (186.50 MHz) and $^{19}F\{^1H\}$ (470.53 MHz). The solutions were obtained by dissolving of 5–40 mg of each compound in 0.5 ml of deuterated solvents.

3.3. X-ray crystallography

Data for colorless crystals (Table 1) were collected on a Nonius KappaCCD diffractometer using Mo $K\alpha$ radiation ($\lambda = 0.71073$ Å), and graphite monochromator. The structures were solved by direct methods (SIR92 [24]). All reflections were used in the structure refinement based on F^2 by full-matrix least-squares technique (SHELXL97 [25]). Heavy atoms were refined anisotropically except of bridging fluorine atoms. The highest residual maximum in **3c** is described above as the second position of bridging fluorine (zig-zag chain, and is very low at 100 K). Hydrogen atoms were mostly localized on a difference Fourier map, however to ensure uniformity of treatment of crystal, all hydrogen were recalculated into idealized positions (riding model) and assigned temperature factors $H_{iso}(H) = 1.2\ U_{eq}$(pivot atom) or of $1.5U_{eq}$ for the methyl moiety. Absorption corrections were carried on, using Gaussian integration from crystal shape [26].

3.4. DSC

The DSC measurements were performed on differential scanning calorimeter Pyris 1 (Perkin–Elmer). Calorimeter was carefully calibrated and nitrogen gas of precisely regulated constant flow 20 ml/min was used as a purging gas. Crystalline samples (weight around 4 mg) were encapsulated into aluminium pans and DSC scans were done using heating rate 10 K/min.

3.5. Computations

All geometries were optimised at the B3LYP [20]/LANL2DZ [21,22] level starting from the experimental crystal structures of the compounds using the GAUSSIAN 03 program [27].

Acknowledgements

The financial support of the Science Foundation of the Czech Republic (Grant No. 203/07/0468) and the Ministry of Education of the Czech Republic (Project VZ0021627501) is acknowledged. F.D.P. wishes to acknowledge the Fund for Scientific Research Flanders (Belgium) and the Free University of Brussels (VUB) for continuous support to his research group.

Appendix A. Supplementary material

CCDC 673998, 673999 and 674000 contain the supplementary crystallographic data for **3a**, **3b** and **3c**. These data can be obtained free of charge from The Cambridge Crystallographic Data Centre via www.ccdc.cam.ac.uk/data_request/cif. Comparative tables and figures for situation of **1–3c** in solid state and in gas phase are given. All computed (as *xyz* files) and measured (as cif files) structures are also given. Supplementary data associated with this article can be found, in the online version, at doi:10.1016/j.jorganchem.2008.06.010.

References

[1] [1a] For reviews see: E.F. Murphy, R. Murugavel, H.W. Roesky, Chem. Rev. 97 (1997) 3425–3460;
[1b] B. Jagirdar, E.F. Murphy, H.W. Roesky, Prog. Inorg. Chem. 48 (1999) 351–455;
[1c] H. Dorn, E.F. Murphy, H.W. Roesky, J. Fluorine Chem. 86 (1997) 121–125.
[2] J.L. Wardell, G.M. Spenser, in: R.B. King (Ed.), Encyclopedia of Inorganic Chemistry, vol. 8, Wiley, New York, 1994, p. 4172.
[3] S.S. Al-Juaid, S.M. Dhaher, C. Eaborn, P.B. Hitchcock, J. Organomet. Chem. 325 (1987) 117–127.
[4] H. Reuter, H. Puff, J. Organomet. Chem. 379 (1989) 223–234.
[5] J. Beckmann, D. Horn, K. Jurkschat, F. Rosche, M. Schürmann, U. Zachwieja, D. Dakternieks, A. Duthie, E.K.L. Lim, Eur. J. Inorg. Chem. (2003) 164–174.
[6] U. Kolb, M. Draeger, M. Dargatz, K. Jurkschat, Organometallics 14 (1995) 2827–2834.
[7] M. Mehring, I. Vrasidas, D. Horn, M. Schürmann, K. Jurkschat, Organometallics 20 (2001) 4647–4653.
[8] N. Pieper, C. Klaus-Mrestani, M. Schürmann, K. Jurkschat, M. Biesemans, I. Verbruggen, J.C. Martins, R. Willem, Organometallics 16 (1997) 1043–1052.
[9] N. Pieper, R. Ludwig, M. Schürmann, K. Jurkschat, M. Biesemans, I. Verbruggen, R. Willem, Phosphorus Sulfur Silicon Relat. Elem. 151 (1999) 305–310.
[10] J. Bareš, P. Novák, M. Nádvorník, T. Lébl, R. Jambor, I. Císařová, A. Růžička, J. Holeček, Organometallics 23 (2004) 2967–2972.
[11] [11a] P. Švec, P. Novák, M. Nádvorník, Z. Padělková, I. Císařová, L. Kolářová, A. Růžička, J. Holeček, J. Fluorine Chem. 128 (2007) 1390–1395;
[11b] L. Dostál, R. Jambor, A. Růžička, R. Jirásko, I. Císařová, J. Holeček, J. Fluorine Chem. 129 (2008) 167–172;
[11c] P. Novák, I. Císařová, L. Kolářová, A. Růžička, J. Holeček, J. Organomet. Chem. 692 (2007) 4287–4296.
[12] P. Novák, J. Brus, I. Císařová, A. Růžička, J. Holeček, J. Fluorine Chem. 126 (2005) 1531–1538.
[13] P. Novák, Z. Padělkova, L. Kolářová, J. Brus, A. Růžička, J. Holeček, Appl. Organomet. Chem. 19 (2005) 1101–1108.
[14] P. Novák, Z. Padělková, I. Císařová, L. Kolářová, A. Růžička, J. Holeček, Appl. Organomet. Chem. 20 (2006) 226–232.
[15] S. Chandra, A. Růžička, P. Švec, H. Lang, Anal. Chim. Acta 577 (2006) 91–97.
[16] A. Růžička, V. Pejchal, J. Holeček, A. Lyčka, K. Jacob, Collect. Czech. Chem. Commun. 63 (1998) 977–989.
[17] P. Švec, Z. Padělková, I. Císařová, A. Růžička, J. Holeček, Main Group Metal Chem. (2007) in press.
[18] [18a] F. Perdih, A. Demšar, A. Pevec, S. Petriček, I. Leban, G. Giester, J. Sieler, H.W. Roesky, Polyhedron 20 (2001) 1967–1971;
[18b] A. Pevec, M. Mrak, A. Demšar, S. Petriček, H.W. Roesky, Polyhedron 22 (2003) 575–579.
[19] A. Asadi, P.B. Hitchcock, C. Eaborn, Inorg. Chem. 42 (2003) 4141–4146.
[20] [20a] A.D. Becke, J. Chem. Phys. 98 (1993) 5648–5652;
[20b] C. Lee, W. Yang, R.G. Parr, Phys. Rev. B 37 (1988) 785–789;
[20c] P.J. Stevens, F.J. Delvin, C.F. Chablaoski, M.J. Frisch, J. Phys. Chem. 98 (1994) 11623–11627.
[21] W.R. Wadt, P.J. Hay, J. Chem. Phys. 82 (1985) 270–283.
[22] [22a] M.A. Buntine, V.J. Hall, F.J. Kosovel, E.R.T. Tiekink, J. Phys. Chem. A 102 (1998) 2472–2482;
[22b] M. Ryner, A. Finne, A.-C. Albertsson, H.R. Kricheldorf, Macromolecules 34 (2001) 7281–7287;
[22c] Y. Obora, M. Nakanishi, M. Tokunaga, Y. Tsuji, J. Org. Chem. 67 (2002) 5835–5837;
[22d] Y.-H. Hu, M.-D. Su, J. Phys. Chem. A 107 (2003) 4130–4135;
[22e] K. Peveling, M. Henn, C. Löw, M. Mehring, M. Schürmann, B. Costisella, K. Jurkschat, Organometallics 23 (2004) 1501–1508;
[22f] J. Fischer, M. Schürmann, M. Mehring, U. Zachwieja, K. Jurkschat, Organometallics 25 (2006) 2886–2893.
[23] L. Dostál, R. Jambor, A. Růžička, I. Císařová, J. Holeček, M. Biesemans, R. Willem, F. De Proft, P. Geerlings, Organometallics 26 (2007) 6312–6319.
[24] A. Altomare, G. Cascarone, C. Giacovazzo, A. Guagliardi, M.C. Burla, G. Polidori, M. Camalli, J. Appl. Crystallogr. 27 (1994) 1045–1050.
[25] G.M. Sheldrick, SHELXL-97, A Program for Crystal Structure Refinement, University of Göttingen, Germanyn, 1997.
[26] P. Coppens, in: F.R. Ahmed, S.R. Hall, C.P. Huber (Eds.), Crystallographic Computing, Copenhagen, Munksgaard, 1970, pp. 255–270.
[27] M.J. Frisch, G.W. Trucks, H.B. Schlegel, G.E. Scuseria, M.A. Robb, J.R. Cheeseman, Jr., J.A. Montgomery, T. Vreven, K.N. Kudin, J.C. Burant, J.M. Millam, S.S. Iyengar, J. Tomasi, V. Barone, B. Mennucci, M. Cossi, G. Scalmani, N. Rega, G.A. Petersson, H. Nakatsuji, M. Hada, M. Ehara, K. Toyota, R. Fukuda, J. Hasegawa, M. Ishida, T. Nakajima, Y. Honda, O. Kitao, H. Nakai, M. Klene, X. Li, J.E. Knox, H.P. Hratchian, J.B. Cross, V. Bakken, C. Adamo, J. Jaramillo, R. Gomperts, R.E. Stratmann, O. Yazyev, A.J. Austin, R. Cammi, C. Pomelli, J.W. Ochterski, P.Y. Ayala, K. Morokuma, G.A. Voth, P. Salvador, J.J. Dannenberg, V.G. Zakrzewski, S. Dapprich, A. D. Daniels, M.C. Strain, O. Farkas, D.K. Malick, A.D. Rabuck, K. Raghavachari, J.B. Foresman, J.V. Ortiz, Q. Cui, A.G. Baboul, S. Clifford, J. Cioslowski, B.B. Stefanov, G. Liu, A. Liashenko, P. Piskorz, I. Komaromi, R.L. Martin, D.J. Fox, T. Keith, M.A. Al-Laham, C.Y. Peng, A. Nanayakkara, M. Challacombe, P.M.W. Gill, B. Johnson, W. Chen, M.W. Wong, C. Gonzalez, J.A. Pople, GAUSSIAN 03, Revision B.03, Gaussian, Inc., Wallingford CT, 2004.